

The decagonal quasicrystal $\text{Al}_{65}\text{Co}_{15}\text{Cu}_{20}$ studied by the Mössbauer effect

This article has been downloaded from IOPscience. Please scroll down to see the full text article.

2005 J. Phys.: Condens. Matter 17 6599

(<http://iopscience.iop.org/0953-8984/17/42/001>)

View [the table of contents for this issue](#), or go to the [journal homepage](#) for more

Download details:

IP Address: 129.252.86.83

The article was downloaded on 28/05/2010 at 07:56

Please note that [terms and conditions apply](#).

The decagonal quasicrystal $\text{Al}_{65}\text{Co}_{15}\text{Cu}_{20}$ studied by the Mössbauer effect

Zbigniew M Stadnik^{1,3} and Guowei Zhang²

¹ Department of Physics, University of Ottawa, Ottawa, ON, K1N 6N5, Canada

² Department of Radiation Oncology, University of Maryland, Baltimore, MD 21201, USA

Received 24 June 2005, in final form 16 September 2005

Published 7 October 2005

Online at stacks.iop.org/JPhysCM/17/6599

Abstract

A systematic ^{57}Fe Mössbauer effect study in a varying temperature range between 5.0 and 296.6 K and in an external magnetic field of 9.0 T on a high-quality stable decagonal quasicrystal $\text{Al}_{65}\text{Co}_{15}\text{Cu}_{19.9}\text{Fe}_{0.1}$ is presented. It is shown that the iron atoms are located in two distinct classes of sites. The values of the principal component of the electric field gradient tensor and the asymmetry parameter at these sites are, respectively, $-1.90(10) \times 10^{21} \text{ V m}^{-2}$, $0.97(15)$ and $-3.95(12) \times 10^{21} \text{ V m}^{-2}$, $0.00(17)$. The average quadrupole splitting decreases with temperature as $T^{3/2}$. The vibrations of the Fe atoms are well described by a Debye model, with the Debye temperature of 546(7) K.

(Some figures in this article are in colour only in the electronic version)

1. Introduction

Quasicrystals (QCs) are a new form of matter which differs from the other two known forms, crystalline and amorphous, by possessing a new type of long-range translational order, *quasiperiodicity*, and a noncrystallographic orientational order associated with the classically forbidden fivefold (icosahedral), eightfold (octagonal), tenfold (decagonal), and twelvefold (dodecagonal) symmetry axes [1]. A central problem in studies of QCs is to determine their atomic structure, which is a prerequisite in understanding many unusual physical properties of these alloys. In spite of significant progress in recent years, the complete determination of the structure of QCs has not yet been accomplished [2].

Since He *et al* [3] and Tsai *et al* [4] found a stable and highly ordered decagonal QC $\text{Al}_{65}\text{Co}_{15}\text{Cu}_{20}$, the decagonal Al–Co–Cu phases have been intensively studied. The decagonal QCs combine two structural characteristics: the atoms are ordered quasiperiodically in planes which are stacked with translational periodicity [1]. The electrical resistivity measurements revealed [5–8] that the electrical resistivity in the periodic direction, ρ_p , is of metallic type (i.e., $\partial\rho/\partial T$ is positive) and that in the quasiperiodic plane, ρ_q , exhibits a nonmetallic behaviour (negative $\partial\rho/\partial T$), similar to that observed in icosahedral QCs, with $\rho_q/\rho_p \gg 1$.

³ Author to whom any correspondence should be addressed.

Anisotropies in the Hall effect [9], thermopower [5], thermal conductivity [10, 11], and optical conductivity [12] have also been observed. The decagonal Al–Co–Cu QCs were also shown to be diamagnetic over a wide temperature range [6, 8, 13]. The physical properties of the decagonal Al–Co–Cu QCs have been interpreted qualitatively by invoking the Hume-Rothery mechanism [7, 9, 11, 13], although optical conductivity [12] and photoemission [14] experiments could not be reconciled with the existence of the pseudogap near the Fermi level. Soft x-ray emission and absorption spectroscopy studies [15] were interpreted as evidence of the presence of a pseudogap in the decagonal Al–Co–Cu alloy. This was later confirmed by ultrahigh-energy resolution photoemission studies of this QC [16].

The first, and until now, the only quantitative x-ray diffraction (XRD) study of the structure of the single-grain decagonal Al–Co–Cu QC using the five-dimensional description of the structure of a single-grain decagonal QC was carried out by Steurer and Kuo [17]. The problem with the five-dimensional approach is that only an average structure can be determined. This is due to the fact that disorder, which is clearly present in the decagonal Al–Co–Cu QC [18], cannot be treated properly. The relatively small number of Bragg reflections available [2] leads to some spurious atoms with unphysical interatomic separations in structural models. In addition, a problem of XRD analysis is that it is not possible to distinguish between the different transition metal (TM) atoms in the ternary Al–Co–Cu QC. It appears that the XRD investigations alone might not be able to solve the structure of the decagonal Al–Co–Cu QC.

The first models of the structure of a decagonal Al–Co–Cu QC based on decorated quasiperiodic tilings were those of Burkov: the initial model was based on a cluster decoration of a Penrose tiling [19] and the later model was based on a decoration of the Tübingen triangular tiling [20]. The Burkov models were compatible with the XRD data of Steurer and Kuo [17] and have been extensively used as the basis for the calculations of the electronic structure of the decagonal Al–Co–Cu QC [21]. Other structural models of the decagonal Al–Cu–Co QC were proposed [22] but have not been pursued further. Recently, total-energy calculations, based on pair potentials derived from first-principles electronic structure considerations and using a minimum of experimental XRD information, have been employed to predict the structure of the decagonal Al–Co–Cu QC [23]. The model is based on tiling of space by hexagonal, boat, and star tiles decorated deterministically with atoms [23].

Complementary to the above discussed methods of structure determination are the local probes, such as extended x-ray absorption fine structure (EXFAS), nuclear quadrupole resonance (NQR), or Mössbauer spectroscopy (MS), which are element selective and sensitive to the local atomic structure. It has been recently demonstrated [24] how the combination of the complete set of the MS data and the calculations of the electric field gradients (EFGs) for several XRD-based structural models of the icosahedral Al–Cu–Fe QC led to the solution of the structure of this QC. Based on the original Burkov model [19], Kramer *et al* [25] calculated the zero-field ^{57}Fe Mössbauer spectrum of the decagonal Al–Cu–Co QC which turned out to be completely different from the experimental spectrum [26, 27]. Similar calculations [28] carried out for various variants of the Burkov model produced ^{57}Fe Mössbauer spectra differing significantly from the experimental one [26, 27].

The main objective of the present study is to provide a complete set of the EFG parameters at the Cu sites in the decagonal Al–Cu–Co QC.

2. Experimental procedure

An ingot of nominal composition $\text{Al}_{65}\text{Co}_{15}\text{Cu}_{19.9}\text{Fe}_{0.1}$ was prepared by melting in an argon atmosphere of high-purity constituent elements using an arc furnace; the Fe metal used was enriched to 95.9% in the ^{57}Fe isotope. The Fe atoms are believed to substitute on the Cu

sites due to the closeness of the metallic radii of Cu (1.28 Å) and Fe (1.27 Å). The ingot was annealed in vacuum at 1073 K for 48 h.

XRD data were collected at 298 K in Bragg–Brentano geometry using a PANalytical X'Pert diffractometer equipped with a PW3020 vertical goniometer with a 173 mm radius and with a long fine-focus Cu target x-ray tube operated at 45 kV and 40 mA. The diffractometer was equipped with a variable divergence slit which kept the illuminated length of the sample constant at 12.5 mm. XRD data were collected by step scanning in the 2θ range 5° – 130° with a step size of 0.02° and a count time of 9 s/step. A fine sample powder was mixed with methanol and allowed to dry on a low-background sample holder, resulting in a thin flat sample. A sample spinner was used to minimize a possible preferred sample orientation. Corrections for instrumental aberration and specimen displacement were made on 2θ angles from the scan of a specimen containing the Si internal standard (National Institute of Standards and Technology reference material 640c). Cu $K\alpha$ radiation was employed and the $K\beta$ line was eliminated by using a Kevex PSi2 Peltier cooled Si detector.

^{57}Fe MS measurements were performed in the temperature range 5.0–296.6 K using a standard Mössbauer spectrometer operating in a sine mode and a source of $^{57}\text{Co}(\text{Rh})$ at room temperature. Mössbauer spectra in an external magnetic field of 9.0 T parallel to the γ -ray propagation direction were measured with the $^{57}\text{Co}(\text{Rh})$ source held at the same temperature as that of the sample. The spectrometer was calibrated with a $6.35\ \mu\text{m}$ α -Fe foil (with a surface density of $107 \times 10^{-3}\ \text{mg}\ ^{57}\text{Fe}/\text{cm}^2$) [29], and the spectra were folded. The full linewidth at half maximum of the inner pair of the α -Fe Zeeman pattern was $0.2244(40)\ \text{mm}\ \text{s}^{-1}$ and this value can be regarded as the resolution of the Mössbauer spectrometer. The Mössbauer absorber was prepared by mixing the powdered alloy with powdered BN to ensure a uniform thickness of the absorber and the random orientation of sample particles. This mixture was then put into a plastic sample holder. The surface density of the Mössbauer absorber was $36 \times 10^{-3}\ \text{mg}\ ^{57}\text{Fe}/\text{cm}^2$.

3. Results and discussion

3.1. Structural characterization

The XRD spectrum of the studied alloy measured in the 2θ range 5° – 130° (figure 1) shows the presence of 46 Bragg peaks due to the decagonal structure and four weak peaks due to an unidentified second phase. The positions of all detected Bragg peaks due to the decagonal structure corresponding to Cu $K\alpha_1$ radiation (the value of its wavelength λ currently accepted by the National Institute for Standards and Technology is $1.540\,5981\ \text{\AA}$ [30]) in terms of the angle $2\theta_1$ and the corresponding wavenumber $Q_{\text{exp}} = 4\pi \sin \theta_1/\lambda$, as well as their relative intensities and full widths at half maximum Γ_Q , were determined from profile fitting using the procedure described in [31], and are given in table 1. The Bragg peaks have been indexed following the scheme of Yamamoto and Ishihara [32]. Table 1 also contains the theoretical positions Q_{cal} , which were calculated by taking the positions of peak numbers 12 and 45 as reference positions, as well as the indices of all Bragg peaks. This analysis yields a quasilattice parameter $a = 7.185\ \text{\AA}$ perpendicular to the tenfold axis and a quasilattice stacking periodicity $c = 4.129\ \text{\AA}$ along the tenfold axis.

There is an excellent agreement between the observed Q_{exp} and the theoretical Q_{cal} positions of the decagonal Bragg peaks (figure 1 and table 1). The widths Γ_Q of most decagonal peaks are found to be limited by the instrumental resolution, which is indicative of a high degree of structural order. The values of the lattice parameters a and c are consistent with the previously published values for the decagonal Al–Cu–Co QC of similar composition [33].

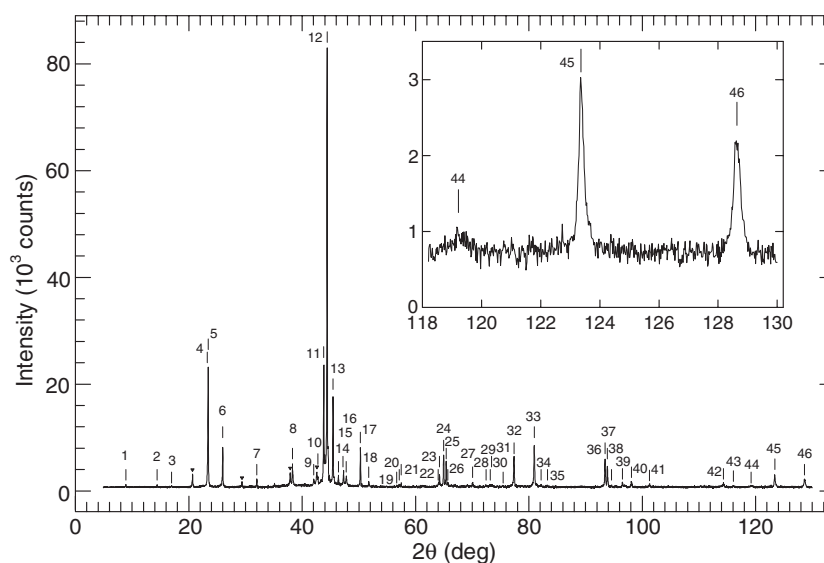


Figure 1. The XRD spectrum of an $\text{Al}_{65}\text{Co}_{15}\text{Cu}_{19.9}\text{Fe}_{0.1}$ alloy at 298 K corrected for the background and the $\text{Cu K}\alpha_2$ lines. The vertical lines labelled with integers above all detected decagonal Bragg peaks correspond to the positions calculated for the $\text{Cu K}\alpha_1$ radiation, as explained in the text. The position, full width at half maximum, and relative intensity of each detected decagonal peak are given in table 1 together with the corresponding index. The symbol \blacktriangledown indicates the peak positions corresponding to an unidentified second phase. The inset shows a part of the spectrum with low-intensity lines.

3.2. Mössbauer spectroscopy

The low-temperature Mössbauer spectrum of the decagonal $\text{Al}_{65}\text{Co}_{15}\text{Cu}_{19.9}\text{Fe}_{0.1}$ QC (figure 2), in contrast to Mössbauer spectra of icosahedral QCs which are in a form of a somewhat broadened single quadrupole doublet [27], exhibits a clear structure. It can be fitted unequivocally with two symmetric quadrupole doublets (figure 2). Each doublet is characterized by a full linewidth at half maximum Γ , a relative area A , a centre shift δ (relative to α -Fe at 298 K), and a quadrupole splitting [34]

$$\Delta = \frac{1}{2}eQ|V_{zz}| \left(1 + \frac{1}{3}\eta^2\right)^{1/2}, \quad (1)$$

where e is the proton charge and Q is the electric quadrupole moment of the nucleus. The asymmetry parameter $\eta = (V_{xx} - V_{yy})/V_{zz}$, ($0 \leq \eta \leq 1$), where V_{xx} , V_{yy} , and V_{zz} are the eigenvalues of the electric field gradient (EFG) tensor in order of increasing magnitude [34]. The values of Γ , A , δ , Δ determined from the fit ($\chi^2 = 1.09$) for each quadrupole doublet are, respectively, $0.313(9) \text{ mm s}^{-1}$, $63.0(2.6)\%$, $0.299(2) \text{ mm s}^{-1}$, $0.389(7) \text{ mm s}^{-1}$ and $0.258(10) \text{ mm s}^{-1}$, $37.0(2.5)\%$, $0.235(3) \text{ mm s}^{-1}$, $0.706(7) \text{ mm s}^{-1}$. The fact that the Mössbauer spectrum of the decagonal $\text{Al}_{65}\text{Co}_{15}\text{Cu}_{19.9}\text{Fe}_{0.1}$ QC is indisputably composed of two quadrupole doublets (figure 2) proves the existence of two distinct iron sites in this QC.

The fit of the zero-field Mössbauer spectrum in figure 2 gives information on the magnitude of Δ , but not on the sign of the main component of the EFG, V_{zz} , or the value of η . The complete information of the sign of V_{zz} and the value of η can be obtained from the Mössbauer spectra measured in external magnetic fields such that the magnetic dipole interaction becomes of a similar magnitude as the electric quadrupole interaction. To determine the sign of V_{zz} and the value of η in the studied QC, a Mössbauer spectrum was measured in an external magnetic field

Table 1. Positions in terms of $2\theta_1$ (in degrees) corresponding to Cu $K\alpha_1$ radiation and Q_{exp} (in \AA^{-1}), full width at half maximum Γ_Q (in \AA^{-1}), and relative intensity INT normalized to 100.0 of all detected decagonal Bragg peaks, which are labelled with consecutive integers in column 1, as obtained from the fit [31]. The integers correspond to the vertical lines in figure 1. Q_{cal} (in \AA^{-1}) is the calculated Q value by taking the positions of peak numbers 12 and 45 as reference positions. Index refers to indices of the decagonal Bragg peaks based on the indexing scheme of Yamamoto and Ishihara [32].

Label	$2\theta_1$	Q_{exp}	Q_{cal}	Γ_Q	INT	Index
1	8.904	0.633	0.633	0.011	0.8	00110
2	14.423	1.024	1.024	0.008	0.7	01210
3	16.970	1.204	1.204	0.009	0.4	01220
4	23.329	1.649	1.648	0.011	10.1	00111
5	23.428	1.656	1.657	0.007	23.9	02320
6	25.983	1.834	1.834	0.009	10.3	01211
7	32.016	2.249	2.249	0.009	2.0	02321
8	38.305	2.676	2.675	0.012	8.3	02431
9	42.064	2.927	2.930	0.011	2.6	00630
10	42.790	2.976	2.975	0.007	1.3	14521
11	43.814	3.043	3.044	0.007	17.7	00002
12	44.405	3.082	3.082	0.007	100.0	03531
13	45.451	3.151	3.151	0.008	20.4	15630
14	46.399	3.213	3.213	0.008	1.9	02621
15	47.213	3.266	3.271	0.018	5.7	00810
16	47.785	3.304	3.306	0.014	6.1	01730
17	50.275	3.465	3.465	0.008	8.9	02322
18	51.756	3.560	3.560	0.007	1.4	15740
19	56.669	3.871	3.872	0.007	0.5	15741
20	57.098	3.898	3.898	0.014	0.9	37860
21	57.474	3.922	3.923	0.007	0.4	12911
22	64.002	4.323	4.323	0.010	1.0	00722
23	64.245	4.337	4.337	0.007	3.7	05850
24	64.971	4.381	4.381	0.008	9.0	15632
25	65.418	4.408	4.408	0.008	7.7	16841
26	65.733	4.427	4.426	0.009	0.9	03642
27	70.066	4.682	4.684	0.011	1.7	00771
28	72.430	4.819	4.819	0.007	0.7	38941
29	73.200	4.863	4.863	0.016	1.2	05960
30	73.416	4.876	4.878	0.009	1.0	02880
31	75.477	4.992	4.992	0.006	0.3	28941
32	77.375	5.099	5.099	0.008	10.5	28 10 50
33	80.946	5.295	5.294	0.010	17.6	03533
34	82.171	5.361	5.360	0.006	0.5	26 11 61
35	83.270	5.419	5.420	0.005	0.3	04990
36	93.430	5.938	5.938	0.008	7.8	00663
37	93.843	5.958	5.958	0.008	7.5	18 11 61
38	94.584	5.994	5.994	0.006	0.6	07 11 70
39	96.537	6.087	6.087	0.007	1.0	00004
40	98.118	6.162	6.162	0.009	2.6	04 10 72
41	101.308	6.308	6.309	0.009	1.4	02324
42	114.329	6.854	6.854	0.010	1.6	15634
43	116.052	6.919	6.920	0.013	0.7	28 13 42
44	119.221	7.036	7.036	0.025	1.9	3 10 14 41
45	123.364	7.181	7.181	0.008	6.8	08 13 81
46	128.636	7.351	7.351	0.009	6.0	25954

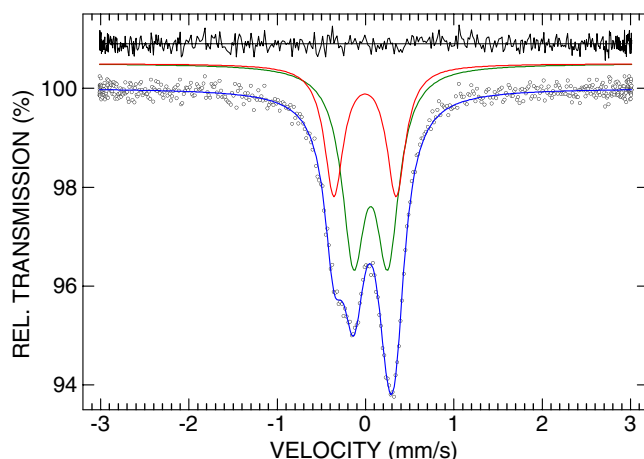


Figure 2. The ^{57}Fe Mössbauer spectrum of the decagonal $\text{Al}_{65}\text{Co}_{15}\text{Cu}_{19.9}\text{Fe}_{0.1}$ quasicrystal at 5.0 K fitted (solid curve) with two symmetric quadrupole doublets. The zero of the velocity scale is relative to the $^{57}\text{Co}(\text{Rh})$ source at 5.0 K. The residuals are shown above the spectrum.

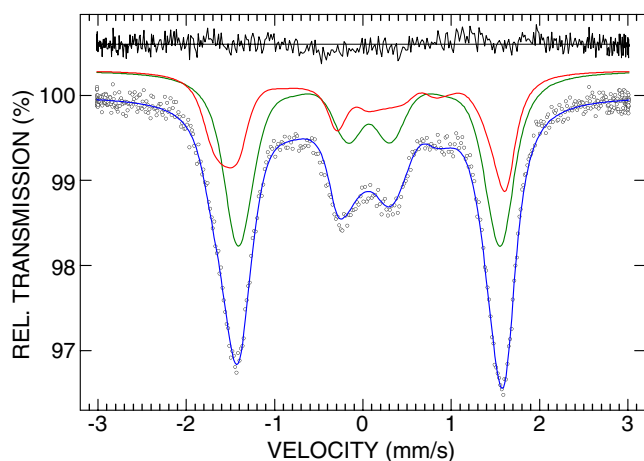


Figure 3. The ^{57}Fe Mössbauer spectrum of the decagonal $\text{Al}_{65}\text{Co}_{15}\text{Cu}_{19.9}\text{Fe}_{0.1}$ quasicrystal at 5.0 K in an external magnetic field of 9.0 T fitted (solid line) with two components. The zero velocity scale is relative to the $^{57}\text{Co}(\text{Rh})$ source at 5.0 K. The residuals are shown above the spectrum.

of 9.0 T (figure 3). The Mössbauer spectra exhibiting mixed hyperfine magnetic dipole and electric quadrupole interactions must be treated using the exact Hamiltonian [34]. If texture effects are negligible one can assume, similarly to the case of powder samples, that the principal axes of the EFG tensor are randomly oriented with respect to the external magnetic field. The algorithm for calculating the spectra in such a case was given by Blaes *et al* [35] and was used to fit the spectrum in figure 3. As there are two classes of iron sites (figure 2), it is clear that there are four possible combinations of signs for $q = \frac{1}{2}eQV_{zz}$: (+, +), (+, -), (-, -), and (-, +). The Mössbauer spectrum in figure 3 was fitted with two components corresponding to these four combinations of q signs; the value of Γ of two component subspectra was taken from the zero-field fit (figure 2) and was fixed in the fit. The best fit ($\chi^2 = 1.24$)

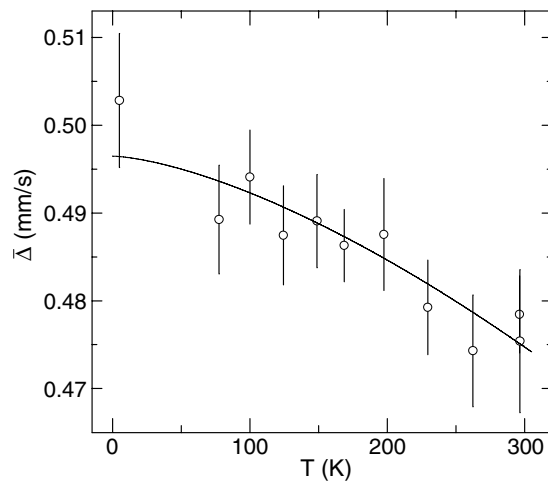


Figure 4. The temperature dependence of the average quadrupole splitting of the decagonal Al₆₅Co₁₅Cu_{19.9}Fe_{0.1} quasicrystal. The solid line is the fit to equation (2), as explained in the text.

(figure 3) was obtained for the following values of A , δ , q , η corresponding, respectively, to two iron sites: 59.5(2.7)%, 0.312(10) mm s⁻¹, -0.316(13) mm s⁻¹, 0.97(15) and 39.5(2.6)%, 0.236(12) mm s⁻¹, -0.658(15) mm s⁻¹, 0.00(17). Thus, V_{zz} is negative at two iron sites and has the value of $-1.90(10) \times 10^{21}$ and $-3.95(12) \times 10^{21}$ V m⁻². In converting from the measured q to V_{zz} we have used the value $Q = 16$ fm², which is based on a systematic comparison of experimentally determined quadrupole splittings and calculated EFGs [36] and which has been confirmed by nuclear shell-model calculations [37].

The analysis presented above enabled us to determine precisely the values of the EFG at the two classes of iron sites in the decagonal Al₆₅Co₁₅Cu_{19.9}Fe_{0.1} QC. What is now required are *ab initio* calculations of the EFGs for the Al-Cu-Co QC for several available structural models [17–20, 22, 23] of this QC. Comparing these calculated EFGs with the experimentally determined EFG here, similarly as has been done for the icosahedral Al-Cu-Fe QC [24], could lead to the solution of the structure of the decagonal Al-Co-Cu QC.

⁵⁷Fe Mössbauer spectra of the decagonal Al₆₅Co₁₅Cu_{19.9}Fe_{0.1} QC were measured at other temperatures. They all exhibit the same two-component structure observed in the spectrum at 5.0 K (figure 2). As a general trend, the average value of the quadrupole splitting $\bar{\Delta}$ decreases with increasing temperature. The temperature dependence of $\bar{\Delta}$ could be fitted (figure 4) to the empirical equation

$$\bar{\Delta}(T) = \bar{\Delta}(0)(1 - BT^{3/2}), \quad (2)$$

where $\bar{\Delta}(0)$ is the value of $\bar{\Delta}$ at 0 K and B is a constant. Such a $T^{3/2}$ temperature dependence has been observed in many metallic noncubic crystalline alloys [38], in some amorphous [39, 40] alloys, and recently in icosahedral QCs [40, 41] over temperature ranges from a few kelvin to the melting point. This seemingly universal $T^{3/2}$ dependence is not well understood. Its origin seems to be associated with a strong temperature dependence of mean-square lattice displacements and, to a lesser extent, with the temperature dependence of lattice expansion [42]. The values of $\bar{\Delta}(0)$, B determined from the fit for the decagonal Al₆₅Co₁₅Cu_{19.9}Fe_{0.1} QC are 0.4965(24) mm s⁻¹, $8.43(1.53) \times 10^{-6}$ K^{-3/2}. The value of B is similar to that found for other metallic amorphous and icosahedral alloys [39–41].

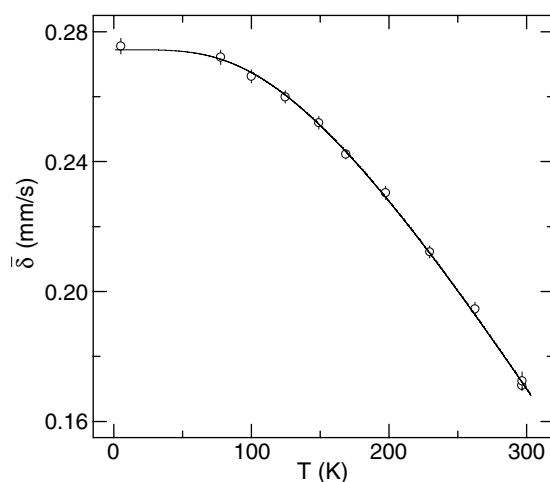


Figure 5. The temperature dependence of the average centre shift of the $\text{Al}_{65}\text{Co}_{15}\text{Cu}_{19.9}\text{Fe}_{0.1}$ quasicrystal. The solid line is the fit to equation (3), as explained in the text.

The average centre shift at temperature T , $\bar{\delta}(T)$, determined from the fits of the spectra of the studied sample measured at different temperatures is given by

$$\bar{\delta}(T) = \delta_0 + \delta_{\text{SOD}}(T), \quad (3)$$

where δ_0 is the intrinsic isomer shift and $\delta_{\text{SOD}}(T)$ is the second-order Doppler (SOD) shift which depends on lattice vibrations of the Fe atoms [34]. In terms of the Debye approximation of the lattice vibrations, $\delta_{\text{SOD}}(T)$ is expressed [34] by the Debye temperature, Θ_D , as

$$\delta_{\text{SOD}}(T) = -\frac{9}{2} \frac{k_B T}{Mc} \left(\frac{T}{\Theta_D} \right)^3 \int_0^{\Theta_D/T} \frac{x^3 dx}{e^x - 1}, \quad (4)$$

where M is the mass of the Mössbauer nucleus and c is the speed of light. By fitting the experimental data $\bar{\delta}(T)$ (figure 5) to equation (3), the quantities δ_0 and Θ_D were found to be, respectively, $0.2745(7) \text{ mm s}^{-1}$ and $546(7) \text{ K}$. The value of Θ_D found here differs significantly from the values of 22 K [7] and 400 K [6] reported for the decagonal $\text{Al}_{65}\text{Cu}_{15}\text{Co}_{20}$ QC, 700 K [8] reported for the decagonal $\text{Al}_{63.2}\text{Cu}_{19.5}\text{Co}_{17.3}$ QC, and is comparable to the value of 596 K [11] found for the decagonal $\text{Al}_{65}\text{Cu}_{15}\text{Co}_{20}$ QC. The values of Θ_D for stable decagonal QCs [11, 43] are significantly larger than those for stable icosahedral QCs [41].

4. Conclusions

A systematic ^{57}Fe Mössbauer effect study in varying temperature range between 5.0 and 296.6 K and in an external magnetic field of 9.0 T on a high-quality stable decagonal quasicrystal $\text{Al}_{65}\text{Co}_{15}\text{Cu}_{19.9}\text{Fe}_{0.1}$ has been presented. The iron atoms are shown to be located in two distinct classes of sites. The values of the principal component of the electric field gradient tensor and the asymmetry parameter at these sites are determined to be, respectively, $-1.90(10) \times 10^{21} \text{ V m}^{-2}$, $0.97(15)$ and $-3.95(12) \times 10^{21} \text{ V m}^{-2}$, $0.00(17)$. The average quadrupole splitting is shown to decrease with temperature as $T^{3/2}$. The vibrations of the Fe atoms are well described by a Debye model, with the Debye temperature of $546(7) \text{ K}$, which is considerably higher than the Debye temperatures previously reported for stable icosahedral quasicrystals.

Acknowledgment

This work was supported by the Natural Sciences and Engineering Research Council of Canada.

References

- [1] Stadnik Z M (ed) 1999 *Physical Properties of Quasicrystals* (Berlin: Springer)
- [2] Steurer W 2004 *J. Non-Cryst. Solids* **334/335** 137
- [3] He L X, Wu Y K and Kuo K H 1988 *J. Mater. Sci. Lett.* **7** 1284
- [4] Tsai A-P, Inoue A and Masumoto T 1989 *Mater. Trans. JIM* **30** 300
Tsai A-P, Inoue A and Masumoto T 1989 *Mater. Trans. JIM* **30** 463
- [5] Lin S-Y, Wang X-M, Lu L, Zhang D-L, He L X and Kuo K X 1990 *Phys. Rev. B* **41** 9625
- [6] Martin S, Hebard A F, Kortan A R and Thiel F A 1991 *Phys. Rev. Lett.* **67** 719
- [7] Wang Y-P and Zhang D-L 1994 *Phys. Rev. B* **49** 13204
- [8] Ribeiro R A, Bud'ko S L, Laabs F C, Kramer M J and Canfield P C 2004 *Phil. Mag.* **21** 1291
- [9] Zhang D-L, Lu L, Wang X-M, Lin S-Y, He L X and Kuo K H 1990 *Phys. Rev. B* **41** 8557
Wang Y-P, Lu L and Zhang D-L 1993 *J. Non-Cryst. Solids* **153/154** 361
Wang Y-P, Zhang D-L and Chen L F 1993 *Phys. Rev. B* **48** 10542
- [10] Zhang D-L, Cao S-C, Wang Y-P, Lu L, Wang X-M, Ma X L and Kuo K H 1991 *Phys. Rev. Lett.* **66** 2778
- [11] Edagawa K, Chernikov M A, Bianchi A D, Felder E, Gubler U and Ott H R 1996 *Phys. Rev. Lett.* **77** 1071
- [12] Basov D N, Timusk T, Barakat F, Greedan J and Grushko B 1994 *Phys. Rev. Lett.* **72** 1937
- [13] Lück R and Kek S 1993 *J. Non-Cryst. Solids* **153/154** 329
- [14] Stadnik Z M, Zhang G W, Tsai A-P and Inoue A 1995 *Phys. Rev. B* **51** 11358
- [15] Belin-Ferré E, Dankházi Z, Fournée V, Sadoc A, Berger C, Müller H and Kirchmayr H 1996 *J. Phys.: Condens. Matter* **8** 6213
- [16] Stadnik Z M, Purdie D, Garnier M, Baer Y, Tsai A-P, Inoue A, Edagawa K, Takeuchi S and Buschow K H J 1997 *Phys. Rev. B* **55** 10938
Stadnik Z M 2001 *Mater. Trans. JIM* **42** 920
- [17] Steurer W and Kuo K H 1990 *Acta Crystallogr. B* **46** 703
Steurer W and Kuo K H 1990 *Phil. Mag. Lett.* **62** 175
- [18] Frey F and Steurer W 1993 *J. Non-Cryst. Solids* **153/154** 600
- [19] Burkov S E 1991 *Phys. Rev. Lett.* **64** 614
Burkov S E 1992 *J. Physique I* **2** 695
- [20] Burkov S E 1993 *Phys. Rev. B* **47** 12325
- [21] Trambly de Laissardière G and Fujiwara T 1994 *Phys. Rev. B* **50** 9843
Sabiryanov R F, Bose S K and Burkov S E 1995 *J. Phys.: Condens. Matter* **7** 5437
Krajčí M, Hafner J and Mihalkovič M 1997 *Phys. Rev. B* **56** 3072
Haerle R and Kramer P 1998 *Phys. Rev. B* **58** 716
Krajčí M and Hafner J 1998 *Phys. Rev. B* **58** 5378
- [22] Daulton T L and Kelton K F 1992 *Phil. Mag. B* **66** 37
Song S G and Ryba E R 1994 *Phil. Mag. B* **69** 707
- [23] Cockayne E and Widom M 1998 *Phys. Rev. Lett.* **81** 598
- [24] Zijlstra E S, Kortus J, Krajčí M, Stadnik Z M and Bose S K 2004 *Phys. Rev. B* **69** 094206
- [25] Kramer P, Quandt A, Schlottmann M and Schneider T 1995 *Phys. Rev. B* **51** 8815
- [26] Eibschütz M, Lines M E, Chen H S and Thiel F A 1992 *Phys. Rev. B* **46** 491
- [27] Stadnik Z M 1996 *Mössbauer Spectroscopy Applied to Magnetism and Materials Science* vol 2, ed G J Long and F Grandjean (New York: Plenum) p 125
- [28] Kramer P, Quandt A, Schneider Th and Teuscher H 1997 *Phys. Rev. B* **55** 8793
Kramer P, Quandt A, Schneider Th and Teuscher H 1998 *Phys. Rev. B* **57** 5542 (erratum)
- [29] Cali J P (ed) 1971 *Certificate of Calibration, Iron Foil Mössbauer Standard* NBS Circular no 1541 (Washington, DC: US Govt Printing Office)
- [30] Jenkins R and Schreiner W N 1989 *Powder Diffr.* **4** 74
- [31] Schreiner W N and Jenkins R 1983 *Adv. X-ray Anal.* **26** 141
- [32] Yamamoto A and Ishihara K N 1988 *Acta Crystallogr. A* **44** 707
- [33] Dong C, Dubois J M, De Boissieu M and Janot C 1991 *J. Phys.: Condens. Matter* **3** 1665
- [34] Greenwood N N and Gibb T C 1971 *Mössbauer Spectroscopy* (London: Chapman and Hall)
Gütlich P, Link R and Trautwein A 1978 *Mössbauer Spectroscopy and Transition Metal Chemistry* (Berlin: Springer)
- [35] Blaes N, Fischer H and Gonser U 1985 *Nucl. Instrum. Methods Phys. Res. B* **9** 201

- [36] Dufek P, Blaha P and Schwarz K 1995 *Phys. Rev. Lett.* **75** 3545
- [37] Martínez-Pinedo G, Schwerdtfeger P, Caurier E, Langanke K, Nazarewicz W and Söhnel T 2001 *Phys. Rev. Lett.* **87** 062701
- [38] Kaufmann E N and Vianden R J 1979 *Rev. Mod. Phys.* **51** 161 and references therein
- [39] Deppe P and Rosenberg M 1983 *Hyperfine Interact.* **15/16** 735
Kopcewicz M, Kopcewicz B and Gonser U 1987 *J. Magn. Magn. Mater.* **66** 79
Mao M, Ryan D H and Altounian Z 1994 *Hyperfine Interact.* **92** 2163
- [40] Stadnik Z M, Saida J and Inoue A 2001 *Ferroelectrics* **250** 297
Stadnik Z M, Rapp Ö, Srinivas V, Saida J and Inoue A 2002 *J. Phys.: Condens. Matter* **14** 6883
- [41] Stadnik Z M, Takeuchi T and Mizutani U 2000 *Mater. Sci. Eng. A* **294–296** 331
Brand R A, Voss J and Calvayrac Y 2000 *Mater. Sci. Eng. A* **294–296** 666
Stadnik Z M, Takeuchi T, Tanaka N and Mizutani U 2003 *J. Phys.: Condens. Matter* **15** 6365
- [42] Jena P 1976 *Phys. Rev. Lett.* **36** 418
Nishiyama K, Dimmling F, Kornrumpf Th and Riegel D 1976 *Phys. Rev. Lett.* **37** 357
Christiansen J, Heubes P, Keitel R, Klinger W, Loeffler W, Sandner W and Witthuhn W 1976 *Z. Phys. B* **24** 177
- [43] Bianchi A D, Bommeli F, Felder E, Kenzelmann M, Chernikov M A, Degiorgi L, Ott H R and Edagawa K 1998 *Phys. Rev. B* **58** 3046